Monte Carlo studies on water and LiF cavity properties for dose-reporting quantities when using x-ray and brachytherapy sources

2016 Phys. Med. Biol. 61 8890

(http://iopscience.iop.org/0031-9155/61/24/8890)

IOP Publishing | Institute of Physics and Engineering in Medicine Physics in Medicine & Biology

Phys. Med. Biol. **61** (2016) 8890–8907 doi:10.1088/1361-6560/61/24/8890

Monte Carlo studies on water and LiF cavity properties for dose-reporting quantities when using x-ray and brachytherapy sources

Isabela Soares Lopes Branco[1], **Paula Cristina Guimarães Antunes**[1], **Gabriel Paiva Fonseca**[2] **and Hélio Yoriyaz**[1]

[1] Instituto de Pesquisas Energéticas e Nucleares—IPEN-CNEN/SP, São Paulo, Brazil
[2] Department of Radiation Oncology (MAASTRO), GROW School for Oncology and Developmental Biology, Maastricht University Medical Center, Maastricht 6201 BN, The Netherlands

E-mail: hyoriyaz@ipen.br

Received 4 April 2016, revised 19 August 2016
Accepted for publication 1 November 2016
Published 2 December 2016

Abstract

Model-based dose calculation algorithms (MBDCAs) are the current tools to estimate dose in brachytherapy, which takes into account heterogeneous medium, therefore, departing from water-based formalism (TG-43). One aspect associated to MBCDA is the choice of dose specification medium since it offers two possibilities to report dose: (a) dose to medium in medium, $D_{m,m}$; and (b) dose to water in medium, $D_{w,m}$. The discussion about the preferable quantity to be reported is underway. The dose conversion factors, DCF, between dose to water in medium, $D_{w,m}$, and dose to medium in medium, $D_{m,m}$, is based on cavity theory and can be obtained using different approaches. When experimental dose verification is desired using, for example, thermoluminescent LiF dosimeters, as in *in vivo* dose measurements, a third quantity is obtained, which is the dose to LiF in medium, $D_{LiF,m}$. In this case, DCF to convert from $D_{LiF,m}$ to $D_{w,m}$ or $D_{m,m}$ is necessary. The objective of this study is to estimate DCFs using different approaches, present in the literature, quantifying the differences between them. Also, dose in water and LiF cavities in different tissue media and respective conversion factors to be able to convert LiF-based dose measured values into dose in water or tissue were obtained. Simple cylindrical phantoms composed by different tissue equivalent materials (bone, lung, water and adipose) are modelled. The phantoms contain a radiation source and a cavity with 0.002 69 cm^3 in size,

which is a typical volume of a disc type LiF dosimeter. Three x-rays qualities with average energies ranging from 47 to 250 keV, and three brachytherapy sources, ^{60}Co, ^{192}Ir and ^{137}Cs, are considered. Different cavity theory approaches for DCF calculations and different cavity/medium combinations have been considered in this study. DCF values for water/bone and LiF/bone cases have strong dependence with energy increasing as the photon energy increases. DCF values also increase with energy for LiF/lung and water/lung cases but, they are much less dependent of energy. For LiF/adipose, water/adipose and LiF/water cases, the DCF values are also dependent of photon energy but, decreases as the energy increases. Maximum difference of 12% has been found compared to values in literature.

Keywords: brachytherapy, cavity theory, Monte Carlo simulation, dose conversion factor

(Some figures may appear in colour only in the online journal)

1. Introduction

Tissue dose calculation in brachytherapy is currently obtained with model-based dose calculation algorithms (MBDCAs) (Rivard *et al* 2009, Beaulieu *et al* 2012). These algorithms have been recently incorporated into commercial treatment planning systems (TPS) and take into account the tissue heterogeneities, applicators and patient-specific characteristics. One aspect associated to MBCDA is the choice of dose specification medium since it offers two possibilities to report dose: (a) dose to medium in medium, $D_{m,m}$ and; (b) dose to water in medium, $D_{w,m}$ (Tedgren and Carlsson 2013, Andreo 2015, Fonseca *et al* 2015). There is no consensus, however, on which dose report quantity should be adopted neither about the method to calculate those quantities (Beaulieu *et al* 2012, Enger *et al* 2012, Thomson *et al* 2013).

The dose conversion factors, DCF, between dose to water in medium, $D_{w,m}$, and dose to medium in medium, $D_{m,m}$, is based on cavity theory and can be obtained using different approaches. When experimental dose verification is desired using, for example, thermoluminescent LiF dosimeters, as *in vivo* dose measurements, a third quantity is obtained, which is the dose to LiF in medium, $D_{LiF,m}$.

The theory that allows such analysis is the cavity theory and the method depends on the size of the target volume or cavity where the dose is calculated. The cavity is considered small or large when its dimension is smaller or larger than the range of secondary electrons. Small cavities satisfy the Bragg–Gray theory where the delivered dose is predominantly due to the charged particles completely traversing the cavity and their fluence is not affected by the presence of the cavity. In this case, the ratio of dose in the cavity and surrounding medium is determined by the mass collision stopping power ratio (Attix 1986). For large cavities, the dose is practically all due to the energy deposited by the charged particles produced inside the cavity. In this case, the dose ratio is obtained considering the ratio of mass-energy absorption coefficients (Borg *et al* 2000, Siebers *et al* 2000, Landry *et al* 2011, Tedgren and Carlsson 2013).

Monte Carlo based computational algorithms have been particularly useful for cavity theory studies due to their precision and flexibility to estimate energy deposition in complex geometries and in a variety of situations, involving heterogeneous materials including the determination of particle fluence in cavities (Rogers 2006). They have also been useful to determine detectors response and verify experimental dose measurements and *in vivo*

dosimetry to predict toxicity due to the radiation exposure (Cortes 2014). Doses received by patients during clinical, diagnostic or therapeutic procedures can be determined by LiF-based thermoluminescent dosimeters placed in specific regions in the body (Knoll 1989, Tedgren *et al* 2011). The dosimeter response should be converted to dose in medium or water, which can be done characterizing the dosimeter as a cavity with typical dimensions of few millimeters in diameter and tenths of millimeter in thickness.

The goal of this work is to investigate the physical parameters involved in the relationship between dose to cavity-in-medium, $D_{c,m}$, and dose to medium-in-medium, $D_{m,m}$ and quantify the respective conversion factors using different approaches, for example, to be able to covert LiF-based dose measured values into dose in water or tissue. For this task, two cavity materials, water and LiF, and four medium materials, mineral bone, adipose, lung and water, have been considered in the analysis.

Cavity is considered in three different approaches: small, medium or large and were treated according to their theories, respectively: SCT—small cavity theory, MCT—medium cavity theory according to the Burlin theory and LCT—large cavity theory (Attix 1986). Six different radiation sources including three x-rays qualities and three typical brachytherapy sources, ^{60}Co, ^{192}Ir and ^{137}Cs, are used.

The choice for water cavity is because, in most of the cases, it is the preferable medium for dose estimates, due to previous clinical experience (Rivard *et al* 2004, Andreo 2015) and LiF cavity is chosen because it is one of the most common dosimeters for *in vivo* dose measurements (Mckeever 1985, Davis *et al* 2003, Nunn *et al* 2008, Tedgren *et al* 2011).

2. Material and methods

2.1. The cavity theory and dose conversion factors

Dose conversion factor (DCF) is obtained as the ratio of the dose in the cavity-in-medium, $D_{c,m}$, and the dose to medium-in-medium, $D_{m,m}$, by the use of the cavity theory. In this study we have:

$$\mathrm{DCF} = \frac{D_{\mathrm{water(or\ LiF),medium}}}{D_{\mathrm{medium,medium}}} \tag{1}$$

The cavity theory that should be used depends on the cavity size. For small cavities, the Spencer–Attix cavity theory (Spencer and Attix 1955) can be used where the DCF is obtained as the ratio of the spectrum averaged mean restricted mass collision stopping power between cavity and medium to take into account the energy deposited by delta-rays given by:

$$\mathrm{DCF} = \left(\frac{\overline{S_{\mathrm{col}}}}{\rho}\right)_{\mathrm{medium}}^{\mathrm{water(or\ LiF)}} \tag{2}$$

For large cavity, the DCF is obtained by the ratio of spectrum averaged mass-energy absorption coefficients of the cavity and medium as (Rivard *et al* 2010, Landry *et al* 2011, Sutherland *et al* 2012):

$$\mathrm{DCF} = \left(\frac{\overline{\mu_{\mathrm{en}}}}{\rho}\right)_{\mathrm{medium}}^{\mathrm{water(or\ LiF)}} \tag{3}$$

Burlin cavity theory for photons covers the situation where the cavity size is not small enough to neglect photon absorption in the cavity and not large enough to neglect the electron

range. The simple relationship that takes into account both situations are given by (Attix 1986):

$$\mathrm{DCF} = d \cdot \left(\frac{\overline{S_{\mathrm{col}}}}{\rho} \right)_{\mathrm{medium}}^{\mathrm{water(or\ LiF)}} + (1 - d) \cdot \left(\frac{\overline{\mu_{\mathrm{en}}}}{\rho} \right)_{\mathrm{medium}}^{\mathrm{water(or\ LiF)}} \tag{4}$$

where $\boldsymbol{d}$ is a weighting factor that considers the cavity size assuming values from zero, for large cavities, up to 1, for small cavities according to the expression:

$$d = \frac{1 - \mathrm{e}^{-\beta L}}{\beta L} \tag{5}$$

where $\boldsymbol{L}$ is the mean chord length for convex cavities and isotropic electron field, which is calculated by four times the cavity volume divided by the cavity surface area.

Assuming that the electron fluence entering the cavity wall decays exponentially as it crosses the medium without changing its energy spectrum (Attix 1986), the parameter β in equation (5) is determined fitting the electron fluence, $\varnothing^{\mathrm{e}}(l)$, as a function of cavity depth, $\boldsymbol{l}$, according to equation (6) below:

$$\varnothing^{\mathrm{e}}(l) = \varnothing_{\mathrm{w}}^{\mathrm{e}}\, \mathrm{e}^{-\beta l} \tag{6}$$

where $\varnothing_{\mathrm{w}}^{\mathrm{e}}$ is the electron fluence in the cavity wall ($l = 0$).

2.2. Monte Carlo simulation

DCFs have been calculated by Monte Carlo (MC) simulations using the MCNP6 code (Goorley *et al* 2013) modelling a cavity with typical dimensions of a disc type thermoluminescent dosimeter (TLD-100) with 0.3 cm in diameter and 0.038 cm in thickness, so that, the scoring volume is 0.002 69 cm^3. The cavity is positioned 1 cm above from the bottom of a cylindrical phantom with dimensions of 4 cm in length and 4 cm in diameter. At 2 cm below the top of the phantom, a 1 cm in diameter disc shaped source is positioned emitting particles in direction to the cavity. The dimensions of the phantom was chosen according to the type of TLD and a simple geometry was preferred since one of the focus of the work was to evaluate the influence of physical parameters involved in the cavity theories to obtain DCF values. This concept follows other works which also preferred simple geometries to perform this type of analysis (Tedgren *et al* 2013). Also, previous simulations to evaluate the effect of phantom dimensions and cavity locations have been done and differences less than 0.5% were observed, for example, increasing the phantom size.

Figure 1 shows the geometric setting of the Monte Carlo modelling used for the simulations. Photons and electrons were transported down to 1 keV with photon cross sections taken from MCPLIB84 library (Goorley *et al* 2013) and electron cross sections from el03 library derived from the ITS3.0 code system (Halbleib *et al* 1992). Four tissue-equivalent materials were used: mineral bone, lung, water and adipose with respective densities of 1.92, 0.38, 1.00 and 0.95 $\mathrm{g \cdot cm^{-3}}$. The atomic composition of each material was taken from ICRP Report 110 (2009) and is presented in table 1. Water was used to represent soft tissue compositions since it is commonly employed for dosimetry purposes and small differences were expected, e.g. differences between water and muscle DCF are very small (Tedgren *et al* 2013, Fonseca *et al* 2015).

Three x-ray beam qualities from ISO-4037N series (Massillon 2014) (NS60, NS80 and NS300) (ISO 1997), and ^{60}Co, ^{192}Ir, and ^{137}Cs gamma sources were used. The photon energies

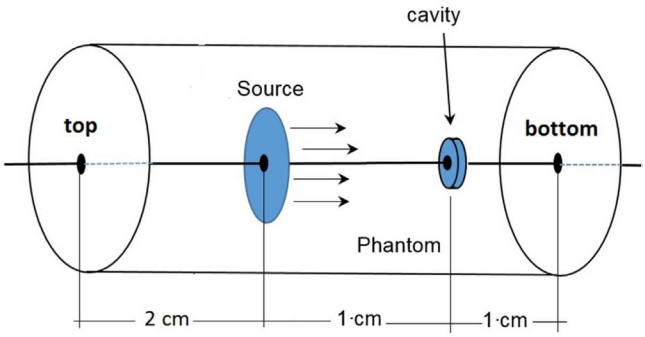

Figure 1. Cylindrical phantom with the radiation source and cavity.

Table 1. Material composition and density of the phantom and cavity.

	Cavity material		Phantom material (tissue-equivalent)		
Element	Water (Nr. atoms)	LiF (Nr. atoms)	Bone (% weight)	Lung (% weight)	Adipose (% weight)
H	2	—	2.2	10.3	11.4
Li	—	1	—	—	—
C	—	—	9.5	10.7	58.8
F	—	1	—	—	—
N	—	—	2.9	3.2	0.8
O	1	—	42.1	74.6	28.7
Na	—	—	—	0.2	0.1
Mg	—	—	0.7	—	—
P	—	—	13.7	0.2	—
S	—	—	—	0.3	0.1
Cl	—	—	—	0.3	0.1
K	—	—	—	0.2	—
Ca	—	—	28.9	—	—
Density ($g \cdot cm^{-3}$)	1.00	2.64	1.92	0.38	0.95

goes from 47 to 1250 keV so the range of secondary electrons, for the different materials evaluated, goes from 2×10^{-3} cm up to 1.5 cm for the 47 keV x-ray source in LiF and ^{60}Co in lung, respectively. Therefore, the TLD dosimeter can be considered a small, intermediate or large cavity depending on the source and material.

2.2.1. DCF for large cavity. DCF(LCT) for large cavity or the mean ratio of the mass energy-absorption coefficient for cavity/medium calculation was performed using the MCNP6 code, through the estimate of the photon energy fluence in the medium, $\psi_{ph}^{medium}(E)$, as follows:

$$\mathrm{DCF(LCT)} = \left(\frac{\overline{\mu_{en}}}{\rho}\right)_{medium}^{cavity} = \frac{\int_0^{E_{max}} \left[\frac{\mu_{en}}{\rho}(E)\right]^{cavity} \cdot \psi_{ph}^{medium}(E)\mathrm{d}E}{\int_0^{E_{max}} \left[\frac{\mu_{en}}{\rho}(E)\right]^{medium} \cdot \psi_{ph}^{medium}(E)\mathrm{d}E} \tag{7}$$

where $\psi_{ph}^{medium}(E) = E \cdot \Phi_{ph}^{medium}(E)$ and $\Phi_{ph}^{medium}(E)$ is the photon fluence in units of particle cm^{-2} and E is the particle energy. In this calculation, the phantom is homogeneous (the cavity material is the same as the medium), so that, the denominator of equation (7) is calculated using track-length estimator (F6 tally) which gives the energy deposition per unit mass (MeV g^{-1}) to the medium (cavity volume) in medium. This tally is based on the average particle track-length, that crosses the target volume and, it is already known from the previous work (Fonseca *et al* 2015), that the values obtained with this tally are consistent with those obtained using $\frac{\mu_{en}}{\rho}$ from National Institute of Standards and Technology (NIST) (Berger 2005). In the same manner, the numerator, which corresponds to the dose to cavity in medium, has been calculated multiplying the energy fluence (*F4 tally) by $\frac{\mu_{en}}{\rho}$ using DE/DF cards. These cards allow one to provide the mass energy-absorption coefficient correspondent to the cavity material in this case, water or LiF, as a function of energy to the MCNP6 code which will utilize it as a response function or flux-to-dose conversion factors.

The influence of the presence of cavity material (LiF or water) on the photon energy fluence and consequently on $\left(\frac{\mu_{en}}{\rho}\right)_{medium}^{cavity}$ has been also analyzed, so that, an alternative calculation of the numerator of equation (7) (heterogeneous case) has been done with F6 tally explicitly using cavity material (LiF or water densities and compositions in the cavity). In this case, the respective photon energy fluence is given by $\psi_{ph}^{cavity(LiF\ or\ water)}(E)$ instead of $\psi_{ph}^{medium}(E)$. In this work, the mass energy-absorption coefficients were taken from NIST tables.

2.2.2. DCF for small cavity. For small cavity, the dose, D(SCT), is obtained considering the restricted mean mass collision stopping power for cavity on the basis of Spencer–Attix cavity theory. Following the methodology proposed by Schaart *et al* (2002), the average absorbed dose in a small volume can be calculated using the electron track-length estimator:

$$D(\mathrm{SCT}) = \int_{\Delta}^{E_{max}} \phi^{e}(E) \cdot \frac{S^{col,\Delta}(E)}{\rho} \mathrm{d}E + D_{\Delta} \tag{8}$$

where ϕ^{e} is the electron fluence (in units of particle cm^{-2}) and $\frac{S^{col,\Delta}}{\rho}$ is the restricted mass-collision stopping power (in units of MeV $\cdot$ cm^2 g^{-1}) excluding the energy transferred to delta particles with energies greater than Δ and D_{Δ} is the track-end contribution to the dose. This last term accounts for the energy deposited by electrons with energy below Δ.

In MCNP6, $\frac{S^{col,\Delta}}{\rho}$ values are provided through DE/DF cards which will be interpolated in a logarithmic energy grid (E_0, E_1,…, E_N), where, E_0 and E_N is respectively, the maximum and minimum photon energy. In this grid, a constant average energy loss per step, ΔE_n ($0 \leqslant n \leqslant N$), is considered to be 8.3%. To account for the track-end contribution, D_{Δ}, the $\frac{S_n^{col,\Delta}}{\rho}$ values at the two lowest energies in the grid, E_N and E_{N-1}, are increased by adding, on average, an energy equivalent to the electron cutoff, E_N, so that:

$$\begin{aligned}
&\frac{S_n^{col,\Delta}(E_n)}{\rho} = \frac{S^{col,\Delta}(E_0)}{\rho} && \text{if } n = 0 \\
&\frac{S_n^{col,\Delta}(E_n)}{\rho} = \frac{S^{col,\Delta}(E_n)}{\rho} && \text{if } 0 < n \leqslant N-1 \\
&\frac{S_n^{col,\Delta}(E_n)}{\rho} = \frac{S^{col,\Delta}(E_n)}{\rho} + \frac{E_N}{T_{N-1}} && \text{if } N-1 \leqslant n \leqslant N
\end{aligned} \tag{9}$$

where T_{N-1} is the correspondent path length (in $g \cdot cm^{-2}$) for the energy step $\Delta E = E_{N-1} - E_N$. The minimum standard electron energy transported in MCNP6 is 1 keV, so that, for the simulations, the values of E_N and Δ were set to this cut-off value.
The dose conversion factor, DCF(SCT), in this case is given by:

$$\mathrm{DCF(SCT)} = \left(\frac{\overline{S_{\mathrm{col}}}}{\rho}\right)^{\mathrm{cavity}}_{\mathrm{medium}} = \frac{\int_{\Delta}^{E_{\max}} \left[\frac{S^{\mathrm{col},\Delta}(E)}{\rho}\right]^{\mathrm{cavity}} \cdot \phi^{\mathrm{e}}_{\mathrm{cavity}}(E)\mathrm{d}E + D_{\Delta}}{\int_{\Delta}^{E_{\max}} \left[\frac{S^{\mathrm{col},\Delta}(E)}{\rho}\right]^{\mathrm{medium}} \cdot \phi^{\mathrm{e}}_{\mathrm{medium}}(E)\mathrm{d}E + D_{\Delta}} \tag{10}$$

As in the previous case, the numerator of equation (10) is calculated for homogeneous and heterogeneous cases to verify the influence of the presence of the cavity material on the electron fluence.

The photon and electron energy spectra shown in this work have been calculated using the track-length estimator, F4, in bins of energy of 1 keV.

2.2.3. Reference values of DCF. Reference values of DCF were calculated transporting secondary electrons and using the MCNP6 energy deposition tally, *F8, which allows one to score dose directly from electron interactions. In contrast with other MCNP6 tallies which are based on particles track-length, the *F8 tally is based on the sampling of particles collision density and the energy deposition is obtained essentially by an analog process. This means that no charged particle equilibrium (CPE) is necessary to account for the energy deposition, but the CPU time necessary to obtain the same statistical precision, as that obtained by track-length estimation could be very high or sometimes unviable depending on the size of the cavity. The reference dose conversion factors using *F8 tally were obtained as the ratio of the dose calculated in the cavity volume (with proper cavity material) and the dose in the cavity with same material as in the medium.

2.2.4. Determination of β parameter. The β parameter in equation (6) has been calculated by Monte Carlo simulation of electron fluence, $\Phi^{\mathrm{e}}(l)$, along the cavity depth, l. For this purpose, the cavity volume was divided into 6 regions along the cavity longitudinal axis, so that, Φ^{e}, could be obtained in each of these regions. The first region is the layer that represents the cavity wall which is facing the radiation beam. The electron fluence in this layer was considered as the wall fluence of electrons, $\phi^{\mathrm{e}}_{\mathrm{w}}$. Figure 2 shows the geometric modelling of the cavity volume divided into 6 regions including the wall layer. Track-length, F4 tally, was used to calculate the electron fluence. The plot of the fluence values considering a homogenous phantom allowed to obtain an exponential fit representing Φ^{e} as a function of depth, l.

β values have also been calculated using Loevinger's formula (Attix 1986) and Burlin suggestions (Burlin 1969) given respectively by:

$$\beta = \frac{16\rho}{(E_{\max} - 0.036)^{1.4}} \tag{11}$$

where ρ is the cavity material density and $E_{\max}$ is the maximum energy of the radiation source; and:

$$\mathrm{e}^{-\beta r_{\max}} = 0.01 \tag{12}$$

where $r_{\max}$ is taken as the maximum electron range ($g \cdot cm^{-2}$). A value of 0.04 suggested by Janssens *et al* (1974), instead of 0.01 in equation (12) was also used considering the observation that it can improve the agreement with experimental results.

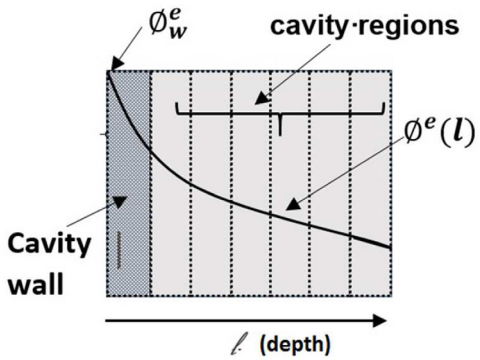

Figure 2. Geometric representation of cavity volume divided in 6 regions along the depth, *l*, where the electron fluence was calculated.

Table 2. Ratio of $\left(\frac{\overline{\mu_{en}}}{\rho}\right)_{medium}^{cavity(LiF\ or\ water)}$ values between homogeneous case (cavity material is the same as the medium material) and heterogeneous case (with explicit cavity material).

		$\frac{\left[\left(\frac{\overline{\mu_{en}}}{\rho}\right)_{medium}^{cavity(LiF\ or\ water)}\right]_{heterogeneous}}{\left[\left(\frac{\overline{\mu_{en}}}{\rho}\right)_{medium}^{cavity(LiF\ or\ water)}\right]_{homogeneous}}$					
Radiation source	Average energy (keV)	Water/ bone	LiF/ bone	Water/ lung	LiF/ lung	Water/ adipose	LiF/ adipose
NS60	47.3	0.992	0.995	0.983	0.988	0.981	0.985
NS80	64.5	0.976	0.977	0.978	0.980	0.976	0.978
NS300	250.5	1.005	1.005	1.007	1.007	1.006	1.006
^{192}Ir	354.7	1.002	1.001	1.003	1.002	1.002	1.002
^{137}Cs	662	1.004	1.002	1.005	1.002	1.005	1.002
^{60}Co	1250	1.002	1.001	1.002	1.002	1.002	0.997

3. Results

3.1. Influence of cavity material on $\left(\frac{\overline{\mu_{en}}}{\rho}\right)_{medium}^{cavity}$

The variation of $\left(\frac{\overline{\mu_{en}}}{\rho}\right)_{medium}^{cavity}$ due to cavity material is shown in table 2. Two sets of configurations are considered: (a) LiF cavity and medium and (b) water cavity and medium. For both situations, water and LiF cavities in medium, the results demonstrate that the presence of cavity material (LIF or water density and composition) influences less than 1% and up to 3% in the $\left(\frac{\overline{\mu_{en}}}{\rho}\right)_{medium}^{cavity}$ values, respectively, for high energy (NS300, ^{192}Ir, ^{137}Cs and ^{60}Co) and low energy (NS60 and NS80) sources. This is in agreement with the behavior of mass-energy absorption coefficients that assume practically the same value above 200 keV, for all materials studied here. On the other hand, for lower energies, <200 keV, the mass-energy absorption coefficients vary for each material and consequently the energy deposition is affected more

Table 3. Ratio of $\left(\frac{\overline{S_{col}}}{\rho}\right)^{cavity}_{medium}$ values.

		$\frac{\left[\frac{(\overline{S_{col}})^{cavity(LiF\ or\ water)}_{medium}}{\rho}\right]_{heterogeneous}}{\left[\frac{(\overline{S_{col}})^{cavity(LiF\ or\ water)}_{medium}}{\rho}\right]_{homogeneous}}$					
Radiation source	Average energy (keV)	Water/ bone	LiF/ bone	Water/ lung	LiF/ lung	Water/ adipose	LiF/ adipose
NS60	47.3	0.046	0.052	0.300	0.447	0.476	0.722
NS80	64.5	0.062	0.062	0.261	0.366	0.348	0.499
NS300	250.5	0.529	0.522	0.622	0.646	0.643	0.669
^{192}Ir	354.7	0.562	0.566	0.659	0.682	0.704	0.708
^{137}Cs	662	0.615	0.624	0.699	0.716	0.638	0.743
^{60}Co	1250	0.654	0.649	0.753	0.799	0.746	0.751

significantly. Also, it has been noticed that higher energy photon fluence suffers little influence on medium heterogeneity, providing no significant changes in the energy deposition in the cavity and consequently in the $\left(\frac{\overline{\mu_{en}}}{\rho}\right)^{cavity}_{medium}$ values.

3.2. *Influence of cavity material on* $\left(\frac{\overline{S_{col}}}{\rho}\right)^{cavity}_{medium}$

In the same manner, the ratio of $\left(\frac{\overline{S_{col}}}{\rho}\right)^{cavity}_{medium}$ values obtained from heterogeneous and homogeneous cases are presented in table 3. Although the little variation of the stopping power ratio with energy between the materials, the exchange of density and composition in the cavity material have great impact on the mean stopping power ratio due to the changes in the electron fluence and particularly for low energy sources like NS60 and NS80. For these two sources and particularly for cavity/bone case the total electron fluence in the homogeneous case are almost 20 times greater than the values obtained in the heterogeneous case.

Figures 3(a)–(d) show the photon and electron spectra in the cavity volume produced by the NS60 x-ray source. Figures 3(a) and (b) show, respectively, the photon and electron spectra, for the homogeneous (water/water) and heterogeneous (LiF/water) cases. Similarly, figures 3(c) and (d) show, respectively, the photon and electron spectra, for the homogeneous (bone/bone) and heterogeneous (water/bone and LiF/bone) cases. The shape of photon spectra does not change with the cavity material and their intensity remains unaltered, however, the intensity of electron spectra in the cavity is very sensitive to the exchange of the cavity material. There is one order of magnitude difference in the electron fluence intensity between bone/bone and water/bone cases.

Although the difference between LiF and water densities being significant (2.64 and 1.00), both cases, water/bone and LiF/bone, provide very close electron fluence values in the cavity as can be observed in figure 3(d).

For higher energy sources like ^{60}Co, the electron fluence for homogeneous case is only 8% higher than for the heterogeneous case. In all cases, the majority contribution to the fluence comes from knock-on electrons. For others two media, lung and adipose, the impact of density and composition of cavity material are still large for low energies, but not as significant as for the bone medium.

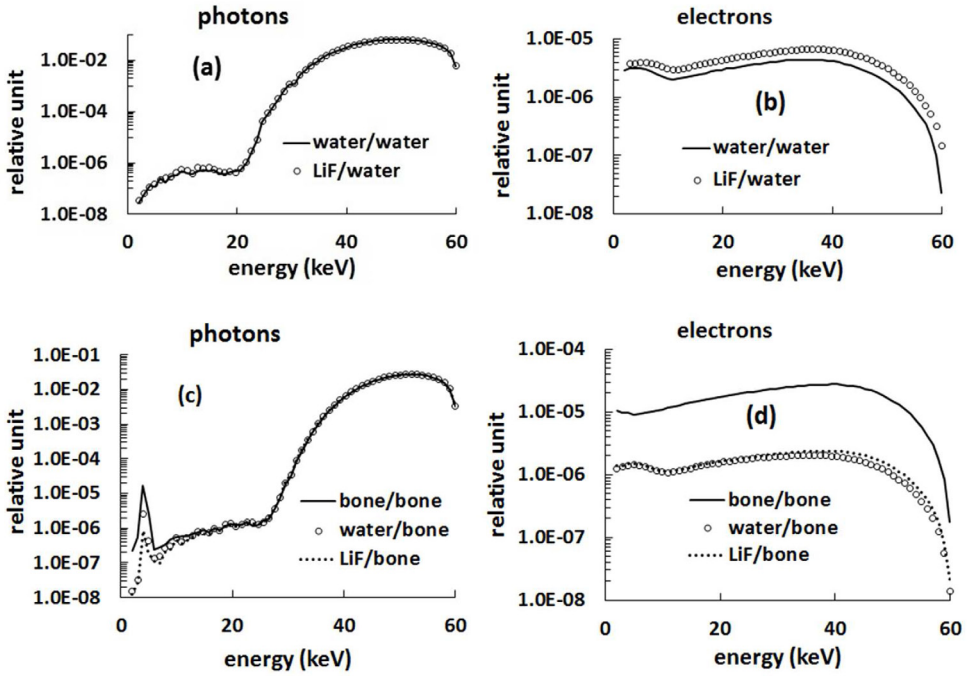

Figure 3. Comparison of photon and electron spectra in the cavity volume due to NS60 x-ray source, for different combinations of cavity/medium materials. Homogeneous case: water/water and bone/bone; Heterogeneous cases: LiF/water, LiF/bone and water/bone.

3.3. β and d values

Figure 4 shows the β values as a function of energy obtained with each approach considered in the present study and the respective values for the parameter d for all set of medium and cavity materials. The β values varies according to different approaches including those obtained by MC simulations. As observed by Tedgren *et al* (2013), values obtained from Loevinger's formula tends to be higher than those obtained using other approaches with increasing relative differences for low energies. β values from MC simulations are within the range of values obtained using Loevinger's and Burlin's approaches. Again, the relative differences increase for low energies, but produce low impact in DCF, since for this range of energy $\boldsymbol{d}$ assumes small values and the cavity can be considered large. For higher energies, the relative differences in β values diminish, d approximates to 1 and the component of small cavity predominates in most of the cases.

3.4. $\left(\frac{\overline{\mu_{en}}}{\rho}\right)^{cavity}_{medium}$ and $\left(\frac{\overline{S_{col}}}{\rho}\right)^{cavity}_{medium}$ values

Figure 5(a) shows $\left(\frac{\overline{\mu_{en}}}{\rho}\right)^{water}_{medium}$ as a function of energy for all medium materials. As can be observed, values are constant for all medium material, except for lower energies, increasing for adipose medium and decreasing for lung medium. The ratios of μ_{en}/ρ taken from NIST tables also present similar behavior, but with slightly lower values. Likewise, figure 5(b) shows $\left(\frac{\overline{\mu_{en}}}{\rho}\right)^{LiF}_{medium}$ as a function of energy for all medium material. For higher energies, the values are constant and

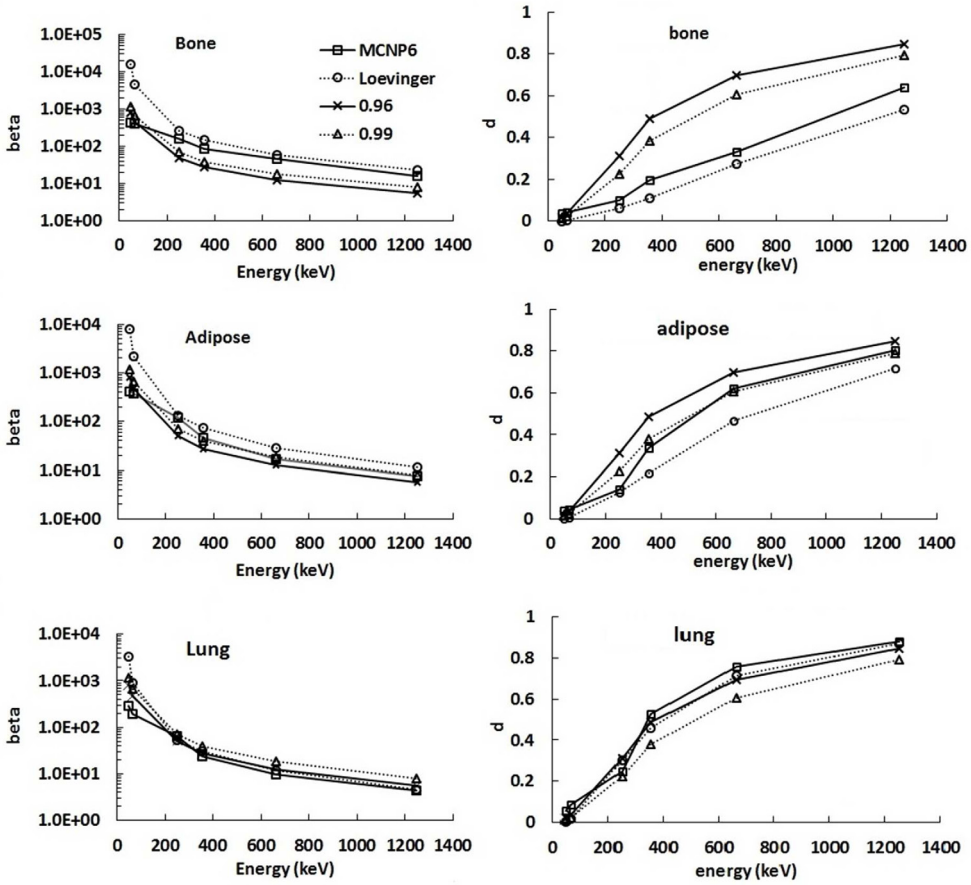

Figure 4. β and d values as a function of source photon energy calculated using 4 different approaches: (a) MCNP6; (b) Loevinger; (c) Janssens (0.96) and (d) Burlin (0.99).

independent of medium material and as expected, for lower energy sources, the results become highly dependent of the cavity/medium materials particularly for NS60 and NS80.

Figures 5(c) and (d) show, respectively, the values of $\left(\frac{\overline{S_{\text{col}}}}{\rho}\right)^{\text{water}}_{\text{medium}}$ and $\left(\frac{\overline{S_{\text{col}}}}{\rho}\right)^{\text{LiF}}_{\text{medium}}$ as a function of energy for all medium materials. The values smoothly decrease as the energy increases except for LiF cavity in water medium, which is almost independent of energy and assume values of 0.8. Results obtained from the ratio of NIST table values demonstrated to be constant in all range of energy covered in this study.

Basically, the differences in the $\left(\frac{\overline{\mu_{\text{en}}}}{\rho}\right)^{\text{cavity}}_{\text{medium}}$ and $\left(\frac{\overline{S_{\text{col}}}}{\rho}\right)^{\text{cavity}}_{\text{medium}}$ behavior obtained here from those obtained as the ratio of μ_{en}/ρ and S_{col}/ρ values taken from NIST tables are due to photon and electron energy spectra variations, respectively, in the cavity, which are taken into account in the calculations.

3.5. DCF values

Tables 4–6 present the dose conversion factors (DCF) obtained for the case where water is the cavity material in bone, lung and adipose media, respectively. For comparison purposes, DCF

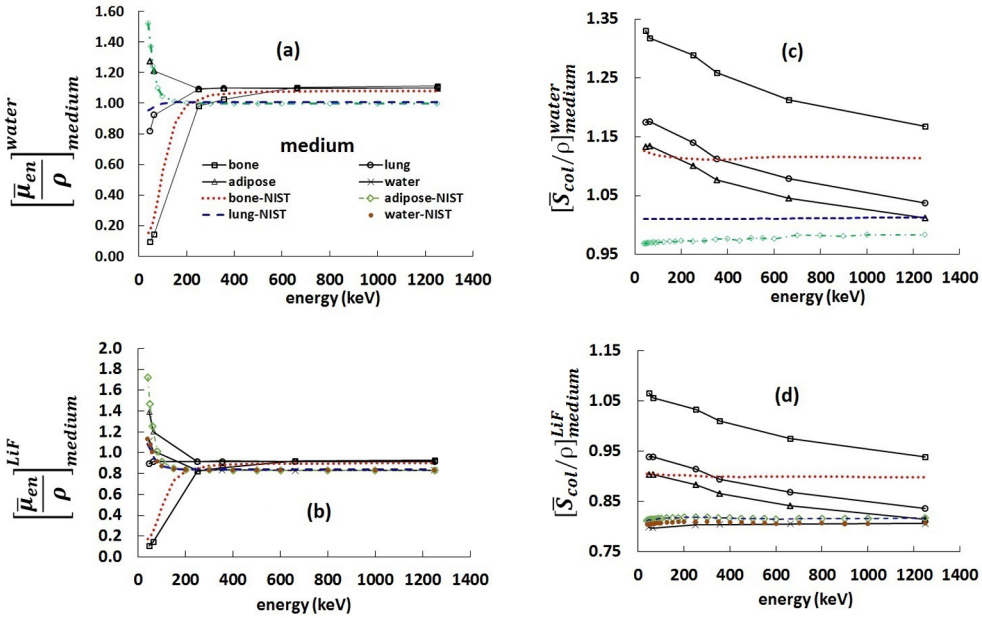

Figure 5. Values of $\left(\frac{\overline{\mu_{\text{en}}}}{\rho}\right)^{\text{cavity}}_{\text{medium}}$ and $\left(\frac{\overline{S_{\text{col}}}}{\rho}\right)^{\text{cavity}}_{\text{medium}}$ as a function of photon source energy. Spectrum averaged mass-energy absorption ratio a) water cavity; b) LiF cavity. Spectrum averaged mean restricted stopping power ratio c) water cavity; d) LiF cavity.

Table 4. Reference DCF values in water cavity and bone medium and respective percentage differences obtained with other approaches.

		Percentage difference (%)					
		DCF(MCT)					
Energy (keV)	Reference DCF water/bone	MCNP6	Loevinger	Janssens	Burlin	DCF(LCT)	DCF(SCT)
47.3	0.134	7.35	−26.34	−8.68	−14.29	−27.29	891.75
64.5	0.202	−3.56	−25.23	−6.95	−13.10	−27.37	554.19
250.5	1.089	−6.99	−8.10	−1.06	−3.49	−9.86	18.39
354.7	1.091	−1.82	−3.68	4.44	2.18	−6.00	15.36
662	1.128	1.04	0.45	4.57	3.68	−2.17	7.51
1250	1.164	−1.36	−1.86	−0.37	−0.64	−4.39	0.35

values calculated by the energy deposition estimated using *F8 energy deposition tally have been adopted as reference values. The percentage differences, (100 ∗ (DCF − Reference)/ Reference), comparing these values with DCF(LCT), DCF(SCT) and DCF(MCT) using four β calculation approaches (MCNP6, Loevinger, Burlin and Janssens) are also shown.

For the water/bone case, table 4, the MCT approach using β values calculated by MCNP6 provided smallest DCF differences in comparison to those provided by other approaches. In this particular case, the LCT and SCT components in equation (4) are weighted by the parameter d, which depends on β values obtained from the best exponential fit of the electron fluence obtained from MCNP6 simulations. The maximum percentage difference is 7.4% occurring for the lowest x-ray energy, NS60, and for the three highest energies, the percentage differences are less than 2%. According to the results in table 4, the cavity can be considered small for ^{60}Co.

Table 5. Reference DCF values in water cavity and lung medium and respective percentage differences obtained with other approaches.

Energy (keV)	Reference DCF water/lung	Percentage difference (%)					
		DCF(MCT)					
		MCNP6	Loevinger	Janssens	Burlin	DCF(LCT)	DCF(SCT)
47.3	0.812	3.26	0.95	1.62	1.35	0.73	44.65
64.5	0.915	3.33	1.42	1.88	1.59	0.91	28.62
250.5	1.108	−0.32	−0.10	−0.05	−0.41	−1.37	2.87
354.7	1.100	0.48	0.38	0.42	0.28	−0.25	1.13
662	1.108	−2.22	−2.14	−2.11	−1.94	−0.81	−2.67
1250	1.159	−9.79	−9.74	−9.61	−9.30	−4.95	−10.45

Table 6. Reference DCF values in water cavity and adipose medium and respective percentage differences obtained with other approaches.

Energy (keV)	Reference DCF water/adipose	Percentage difference (%)					
		DCF(MCT)					
		MCNP6	Loevinger	Janssens	Burlin	DCF(LCT)	DCF(SCT)
47.3	1.245	2.02	2.46	2.25	2.32	2.49	−9.01
64.5	1.183	2.17	2.41	2.23	2.30	2.46	−4.11
250.5	1.102	−0.56	−0.57	−0.47	−0.52	−0.63	−0.12
354.7	1.104	−1.13	−0.88	−1.45	−1.23	−0.42	−2.52
662	1.107	−3.78	−3.06	−4.13	−3.70	−0.88	−5.55
1250	1.117	−7.89	−7.20	−8.21	−7.77	−1.57	−9.41

Table 7. Reference DCF values in LiF cavity and bone medium and respective percentage differences obtained with other approaches.

Energy (keV)	Reference DCF LiF/bone	Percentage difference (%)					
		DCF(MCT)					
		MCNP6	Loevinger	Janssens	Burlin	DCF(LCT)	DCF(SCT)
47.3	0.118	20.05	−9.81	9.97	3.76	−10.65	803.82
64.5	0.162	12.24	−8.71	13.86	6.44	−10.78	551.43
250.5	0.863	−2.37	−3.35	4.24	1.88	−4.88	19.76
354.7	0.882	0.60	−0.91	6.76	4.92	−2.79	14.59
662	0.920	2.03	1.67	4.46	3.97	0.07	5.98
1250	0.927	0.84	0.70	1.17	1.10	−0.05	1.35

For the water/lung case, table 5, the LCT approach provided the smallest differences, so that, the cavity can be considered large. The maximum percentage difference found is 4.95% corresponding to ^{60}Co source. In the same manner, for water/adipose case, table 6, the LCT approach provided the smallest difference with maximum percentage difference of 2.5%.

Tables 7–10 present the dose conversion factors (DCF) obtained in the case where LiF is the cavity material in bone, adipose, lung and water media, respectively. For all cases, except LiF/bone, the smallest percentage differences on DCF values are obtained using the LCT approach. For these cases, the maximum percentage differences are 2.78, 7.02 and

Table 8. Reference DCF values in LiF cavity and adipose medium and respective percentage differences obtained with other approaches.

Energy (keV)	Reference DCF LiF/ adipose	Percentage difference (%)					
		DCF(MCT)					
		MCNP6	Loevinger	Janssens	Burlin	DCF(LCT)	DCF(SCT)
47.3	1.370	0.52	1.89	1.05	1.33	1.97	−34.02
64.5	1.170	1.66	2.60	1.66	2.00	2.78	−22.72
250.5	0.920	−0.76	−0.81	−.68	−1.35	−0.39	−3.88
354.7	0.918	−1.87	−1.10	−3.11	−2.49	0.12	−5.76
662	0.917	−5.15	−3.80	−6.11	−5.45	−0.18	−8.18
1250	0.904	−7.65	−6.55	−8.41	−7.88	1.30	−9.81

Table 9. Reference DCF values in LiF cavity and lung medium and respective percentage differences obtained with other approaches.

Energy (keV)	Reference DCF LiF/ lung	Percentage difference (%)					
		DCF(MCT)					
		MCNP6	Loevinger	Janssens	Burlin	DCF(LCT)	DCF(SCT)
47.3	0.883	1.53	1.25	1.37	1.33	1.24	6.29
64.5	0.895	2.30	2.07	2.18	2.14	2.05	4.94
250.5	0.924	−1.13	−1.15	−1.11	−1.12	−1.16	−1.03
354.7	0.915	−1.04	−0.22	−1.09	−0.83	0.30	−2.24
662	0.915	−3.74	−2.13	−3.67	−3.23	0.27	−5.04
1250	0.986	−14.28	−12.85	−14.23	−13.84	−7.02	−15.27

Table 10. Reference DCF values in LiF cavity and water medium and respective percentage differences obtained with other approaches.

Energy (keV)	Reference DCF LiF/ water	Percentage difference (%)					
		DCF(MCT)					
		MCNP6	Loevinger	Janssens	Burlin	DCF(LCT)	DCF(SCT)
47.3	1.095	0.87	1.95	1.27	1.49	2.01	−27.08
64.5	1.035	−2.58	−1.83	−2.61	−2.33	−1.68	−2.93
250.5	0.871	−4.90	−4.97	−5.78	−5.47	−4.58	−7.82
354.7	0.833	−0.97	−0.59	−1.83	−1.45	0.16	−3.46
662	0.830	−1.66	−1.26	−2.13	−1.88	0.08	−2.89
1250	0.824	−1.54	−1.28	−1.79	−1.64	0.86	−2.17

4.58%, respectively, for LiF/adipose, LiF/lung and LiF/water cases. As for LiF/bone case, the maximum percentage difference is 6.44% using MCT approach with Burlin suggestion for β calculation.

4. Discussion

Material density and composition play an important role in the determination of DCF whose value depends on the cavity/medium combination and energy. For example, the

DCF values for the water/bone and LiF/bone cases have strong dependence with energy, increasing as the photon energy increases. DCF values also increase with energy for LiF/lung and water/lung cases but, they are much less dependent of energy. On the contrary, for the LiF/adipose, LiF/water and water/adipose cases, the DCF values decreases as the energy increases.

Water was used to represent soft tissue compositions since it is commonly employed for dosimetry purposes and small differences were expected, e.g. differences between water and muscle DCF are very small (Tedgren *et al* 2013, Fonseca *et al* 2015).

The reason why different cavity theories were used is that the present investigation covered a broad range of energy that goes from 47 to 1250 keV, which are of interest in brachytherapy. Also, several different materials were used, so that, the range of secondary electrons assume values from 2×10^{-3} cm for 47 keV x-ray source in LiF up to 1.5 cm for ^{60}Co in lung. Therefore, considering the fact that the thickness of the TLD dosimeter is 0.038 cm, it would be small, intermediate or large cavity, depending on the source and material being specified. For example, for water/bone case, the MCT using β value calculated by MCNP6 is the best approach. On the other hand, for water/lung and water/adipose cases, the LCT is the best approach. In cases where LiF is the cavity the best approach is LCT except for LiF/bone case where the best approach is MCT using Burlin suggestion for β.

The heterogeneity effect introduced when a cavity material is different from medium has different impact on the ratio of mean mass-energy absorption coefficients. There are cases where the density ratio ($\rho_{\text{cavity}}/\rho_{\text{medium}}$) of materials is significant, like water/bone case (0.52), providing the same DCF value as that provided by water/adipose case which density ratio is only 1.05. This fact demonstrates that the material composition plays an important role in radiation interaction process and, in this particular case, the effect of the difference in density on the DCF is compensated by the difference in the composition.

Tedgren and Carlsson (2013) calculated DCF(LCT) and DCF(SCT) for water/bone and water/adipose using ^{192}Ir source in a cavity scoring volume of 0.006 28 cm^3. Fonseca *et al* (2015) calculated the DCF values for ^{192}Ir in more realistic scenarios using a heterogeneous voxel-based phantom based on CT images of a head and neck treatment with voxel volumes of 0.0003 cm^3. They observed a range of DCF values depending on the photon spectrum in each voxel with variations of up to $>15\%$. The comparison of these values are presented in table 11 in comparison with values obtained in the present work. The scoring volume used by Tedgren and Carlsson and Fonseca *et al* are respectively 2.3 times greater and 8.9 smaller than that used in the present work. The maximum differences between the values obtained here and reported ones are 12%, 11.1% and 10.4% corresponding to DCF(SCT) values, respectively, for water/bone, water/adipose and water/lung cases.

As mentioned before, changes in photon spectrum causes variations in DCF values up to 15% and it depends on the source-cavity distance, so that, one of the causes for the differences in the DCF(SCT) values obtained here compared to reported ones, can be attributed to the different source-cavity distances and also material compositions considered in those different works. The dependence of DCF value on the local spectra shows that its value for the same material may be different within the patient.

From these observations, we believe that each clinical case should be evaluated individually since the local spectra can change depending on the region and from patient to patient, indicating the necessity of further analysis of the influence of material composition and density to the DCF calculation.

Table 11. Comparison of DCF values obtained for ^{192}Ir source obtained by Fonseca *et al* (2015), Tedgren and Carlsson (2013) and this work.

	DCF(LCT)			DCF(SCT)		
Cavity/medium	Tedgren and Carlsson	Fonseca *et al*	This work	Tedgren and Carlsson	Fonseca *et al*	This work
Water/bone	1.014	1–1.14	1.025	1.127	1.133	1.258
Water/adipose	1.002	1.002–1.010	1.099	0.968	0.980	1.076
Water/lung	—	—	1.097	—	1.008	1.113

MBDCAs capability to handle tissue composition and to report different dose quantities are becoming a reality in the clinic. However, there is no consensus on the dose quantities that should be reported with DCF depending on the local spectra for some tissues and varying within the patient (Fonseca *et al* 2015). Moreover, there are several approaches to calculate DCF that can lead to different results. Therefore, in this work we aimed to quantify these differences in the methodologies to calculate DCF, so that, it can be further applied for clinical cases and dosimetry purposes. Also, this work focused on TLDs since it is a very suitable option for dosimetry which is commonly based in dose to water. The results obtained in this work clarifies some issues necessary to move towards to a tissue related calibration so that the TLD response can be converted to tissue specific dose report quantities.

5. Conclusions

Dose conversion factors (DCFs) have been estimated for several radiation sources with energies ranging from few keV x-ray up to ^{60}Co sources. It has been observed that the classification of cavity in terms of size and consequently the best approach for DCF calculation depends not only on the association of cavity size with the radiation source energy, but also, on the density and composition of the materials involved, which have strong influence on the electron fluence in the cavity. Consequently, DCF becomes a function of several parameters related to radiation source and cavity/medium characteristics and their combination including cavity/medium densities and material compositions. For instance, for water/lung and water/adipose cases the size of cavity studied here can be considered large for all energies. Also, in case where LiF is the cavity material it could be considered large for all medium material except in bone medium where the best approach is MCT.

Acknowledgments

This work was partially supported by Conselho Nacional de Desenvolvimento Científico e Tecnológico (CNPq), grant number 305924/2013-3.

References

Andreo P 2015 Dose to 'water-like' media or dose to tissue in MV photons radiotherapy treatment planning: still a matter of debate *Phys. Med. Biol.* **60** 309–37

Attix F H 1986 *Introduction to Radiological Physics and Radiation Dosimetry* (New York: Wiley)

Beaulieu L *et al* 2012 Report of the task group 186 on model-based dose calculation methods in brachytherapy beyond the TG-43 formalism: current status and recommendations for clinical implementation *Med. Phys.* **39** 6208–36

Berger M J *et al* 2005 *XCOM: Photon Cross Section Database (Version 1.3)* (Gaithersburg, MD: NIST)

Borg J, Carlsson Kawrakow I, Rogers D W O and Seuntjens J P 2000 Monte Carlo study of correction factors for Spencer–Attix cavity theory at photon energies at or above 100 keV *Med. Phys.* **27** 1804–13

Burlin T E and Chan F K 1969 The effect of the wall on the Fricke dosemeter *Int. J. Appl. Radiat. Isot.* **20** 767–75

Chadwick M B 2012 ENDF nuclear data in the physical, biological, and medical sciences *Int. J. Radiat. Biol.* 88 10–4

Cortes J R *et al* 2014 Electron absorbed dose measurements in LINACs by thermoluminescent dosimeters *Appl. Radiat. Isot.* **83** 210–3

Davis S D *et al* 2003 The response of LiF thermoluminescence dosemeters to photon beams in the energy range from 30 kV x rays to ^{60}Co gamma rays *Radiat. Prot. Dosim.* **106** 33–43

Enger S A, Ahnesjo A, Verhaegen F and Beaulieu L 2012 Dose to tissue medium or water cavities as surrogate for the dose to cell nuclei at brachytherapy photon energies *Phys. Med. Biol.* **57** 4489–500

Fonseca G P *et al* 2015 Dose specification for ^{192}Ir high dose rate brachytherapy in terms of dose-to-water-in-medium and dose-to-medium-in-medium *Phys. Med. Biol.* **60** 4565–79

Goorley J T *et al* 2013 Initial MCNP6 release overview—MCNP6 version 1.0 (Los Alamos, NM: Los Alamos National Laboratory)

Halbleib J A *et al* 1992 *ITS Version 3.0: Integrated TIGER Series of Coupled Electron/Photon Monte Carlo Transport Codes SAND91-1634* Sandia National Laboratory

ICRP 2009 *Adult Reference Computational Phantoms* (*ICRP Publication 110*) (Oxford: Elsevier)

ISO 1997 *X and Gamma Reference Radiation for Calibrating Dosemeters and Dose Rate Meters and for Determining Their Response as a Function of Photon Energy—Part 1: Radiation Characteristics and Production Methods* (*ISO Report 4037-1*) (Geneva: International Organization for Standardization)

Janssens A and Eggermont G 1974 Spectrum perturbation and energy deposition models for stopping power ratio calculations in general cavity theory *Phys. Med. Biol.* **19** 619–30

Knoll G F 1989 *Radiation Detection and Measurement* (Hoboken, NJ: Wiley)

Landry G *et al* 2011 The difference of scoring dose to water or tissues in Monte Carlo dose calculations for low energy brachytherapy photon sources *Med. Phys.* **38** 1526–33

Mckeever W S 1985 *Thermoluminescence of Solids* (Cambridge: Cambridge University Press)

Massillon J L G *et al* 2014 Influence of phantom materials on the energy dependence of LiF:Mg,Ti thermoluminescent dosimeters exposed to 20–300 kV narrow x-ray spectra, ^{137}Cs and ^{60}Co photons *Phys. Med. Biol.* **59** 4149–66

Nunn A A *et al* 2008 LiF:Mg,Ti TLD response as a function of photon energy for moderately filtered x-ray spectra in the range of 20–250 kVp relative to ^{60}Co *Med. Phys.* **35** 1859–69

Rivard M J, Beaulieu L and Mourtada F 2010 Enhancements to commissioning techniques and quality assurance of brachytherapy treatment planning systems that use model-based dose calculation algorithms *Med. Phys.* **37** 2645–58

Rivard M J, Venselaar J L and Beaulieu L 2009 The evolution of brachytherapy treatment planning *Med. Phys.* **36** 2136–53

Rivard M J *et al* 2004 Update of AAPM task group no. 43 report: a revised AAPM protocol for brachytherapy dose calculations *Med. Phys.* **31** 633–74

Rogers D W 2006 Fifty years of Monte Carlo simulations for medical physics *Phys. Med. Biol.* **51** R287–301

Schaart D R, Jansen J T and Zoetelief J de Leege P F 2002 A comparison of MCNP4C electron transport with ITS 3.0 and experiment at incident energies between 100 keV and 20 MeV: influence of voxel size, substeps and energy indexing algorithm *Phys. Med. Biol.* **47** 1459–84

Siebers J V, Keall P J, Nahum A E and Mohan R 2000 Converting absorbed dose to medium to absorbed dose to water for Monte Carlo based photon beam dose calculations *Phys. Med. Biol.* **45** 983–95

Spencer L V and Attix F H 1955 A theory of cavity ionization *Radiat. Res.* **3** 239–358

Sutherland J G H *et al* 2012 Model-based dose calculations for ^{125}I lung brachytherapy *Med. Phys.* **39** 4365–77

Tedgren A C and Carlsson G A 2013 Specification of absorbed dose to water using model-based dose calculation algorithms for treatment planning in brachytherapy *Phys. Med. Biol.* **58** 2561–79

Tedgren A C *et al* 2011 Response of LiF:Mg,Ti thermoluminescent dosimeters at photon energies relevant to the dosimetry of brachytherapy (<1 MeV) *Med. Phys.* **38** 5539–50

Thomson R M *et al* 2013 On the biological basis for competing macroscopic dose descriptors for kilovoltage dosimetry: cellular dosimetry for brachytherapy and diagnostic radiology *Phys. Med. Biol.* **58** 1123–50